GA–A25543

SYSTEM UPGRADES TO THE DIII–D FACILITY

by

A.G. KELLMAN for the DIII–D TEAM

AUGUST 2006

GENERAL ATOMICS

DISCLAIMER

GA–A25543

SYSTEM UPGRADES TO THE DIII–D FACILITY

by
A.G. KELLMAN for the DIII–D TEAM

This is a preprint of a paper to be presented at the 24th Symposium on Fusion Technology, September 11–15, 2006, Warsaw, Poland, and to be published in *Fusion Engineering and Design.*

Work supported by
the U.S. Department of Energy
under DE-FC02-04ER54698

GENERAL ATOMICS PROJECT 30200
AUGUST 2006

GENERAL ATOMICS

ABSTRACT

Major upgrades to the DIII–D facility have been performed that significantly enhance the capability of both the DIII–D device and the entire facility. The most significant of these include the rotation of a neutral beam line, installation of a new lower divertor, and a significant set of new and enhanced diagnostics. The upgrades and initial results are presented in this paper.

1. INTRODUCTION

The DIII–D facility has just completed a major set of upgrades to both the tokamak and various subsystems. These upgrades address the fundamental goals of the DIII–D program, i.e. advancing the physics of Advanced Tokamaks, exploring basic fusion physics, and addressing critical issues for ITER. The upgrades were performed during a 12-month shutdown period, referred to as the Long Torus Opening Activity (LTOA) that ended in March 2006.

The major upgrades that were performed during this period included: (1) rotation of one of the four neutral beamlines from the co- to counter-direction; (2) the reduction of the largest known source of non-axisymmetric magnetic error field on DIII–D; (3) the modification of the lower divertor to improve density control in high triangularity double-null divertors; (4) the installation of contoured graphite tiles on the lower centerpost to reduce carbon erosion and improve toroidal uniformity; (5) improvements to the plasma control system (PCS) speed and real time control; (6) more than 20 diagnostic upgrades; and (7) installation of two new cooling towers with capability to handle longer pulses and higher heat loads. Two other major upgrades that were started during that period are the conversion of the electron cyclotron system from three short pulse and three long pulse gyrotrons to six long pulse gyrotrons, and an extension of the pulse capability of the toroidal field. This paper describes the major system enhancements and initial results from the first operating period.

2. SYSTEM UPGRADES

The modification with the most significant impact both programmatically and in terms of affected hardware was the rotation of one of the four neutral beam lines from co- to counter-injection. The major system modification was motivated both because it enables new research areas as well as extends existing research to the regime of low rotation, high beta target plasmas, more relevant to the regime in which ITER is expected to operate.

The DIII–D neutral beam system consists of four neutral beam lines, each with two ion sources capable of delivering up to 2.5 MW of 80 kV deuterium neutral beams. Presently, there are seven power supplies for a total system power of 17.5 MW for 3.5 s and reduced power for longer pulses. Until April 2005, all the neutral beam injection were oriented in the co-direction, i.e. the same direction as the standard plasma current. Rotating two sources to counter-injection allows, for the first time on DIII–D, the decoupling of energy and momentum input. By modulating the beams and controlling the on-off duty cycle, we can continuously vary the momentum input from counter to balanced to full co-injection while keeping the power input constant. A new feedback algorithm, taking into account the injection angle for each ion source and the effectiveness of heating and momentum input for the different sources has been implemented on the DIII–D PCS [1]. It enables independent control of plasma-stored energy and plasma rotation, measured in real time using the charge exchange recombination (CER) system [2]. Figure 1 shows a discharge with varying degrees of co- versus counter-beam injection and thus varying torque input. The data show that the plasma rotation measured by CER follows the net input torque and reverses direction as the sign of the torque reverses. Using this technique, steady-state low rotation plasmas (< 2 kHz) have now been produced on DIII–D.

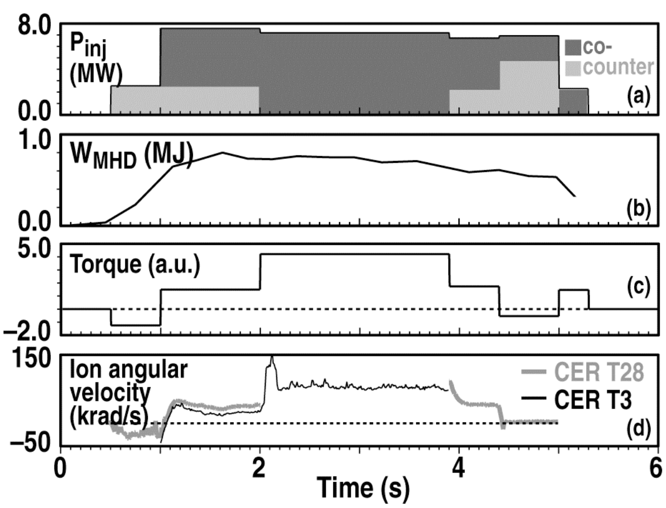

Fig. 1. (a) By varying the mix of co- and counter-beam injection, the net torque (c) applied to the plasma can be reversed and the resulting ion angular velocity (d), as measured by the CER diagnostic follows the applied torque. The stored energy (b) is nearly proportional to the total injected power, but is affected by the mix of co- and counter-beams.

These low rotation plasmas are key elements of the DIII–D research program to investigate important physics issues for ITER. High plasma rotation has been shown to have a strong stabilizing effect on the resistive wall mode (RWM) [3]. However, it is not expected that ITER will have sufficient rotation for rotational stabilization to be effective. Obtaining high beta discharges in DIII–D with rotation frequencies well below the critical rotation frequency for RWM stabilization is essential for testing the effectiveness of stabilization techniques using non-axisymmetric coils. Stabilization of the neoclassical tearing mode (NTM) has also been achieved on DIII–D using Electron Cyclotron Current Drive (ECCD) [4]. To date, only continuous ECCD has been applied to the islands for stabilization. However, this is predicted to be much less effective on ITER where the width of the current drive region is wide compared to the island width. In this regime, modulated ECCD with phased application of the current drive with the island O-point [5] is predicted to be more efficient. Typical NTM island rotation speeds on DIII–D using all co-injection are in excess of 20 kHz, exceeding the modulation capability of our gyrotrons. Using co- and counter-injection, rotation speeds have now been achieved below the 5 kHz required for effective ECCD modulation. In the area of transport studies, balanced injection will permit answering the question of whether the quiescent double barrier (QDB) high energy confinement mode [6] is accessible in ITER-like low rotation discharges. The QDB mode is a very promising mode of operation for ITER because there are no ELM instabilities or high impulsive heat fluxes associated with the ELMs. To date, this mode has only been observed using predominantly counter-injection. By varying the mix of co- and counter-beams, the sensitivity of the mode to the balance of co- and counter-rotation will be investigated.

The rotation of the neutral beamline required a redesign of the feedpoint for the toroidal field (TF). Because the TF bus in the area of the coil feedpoint was known to be the single largest source of non-axisymmetric error field on DIII–D, the geometry of the feed was reworked to significantly reduce the field error. The DIII–D toroidal field coil has 144 turns arranged in 24 bundles of 6 turns. To avoid a vertical field associated with the single toroidal transit through the 144 TF turns, a return bus was incorporated in the original design that canceled the $n = 0$ vertical field. In addition, the interconnecting bus between each of the 24 bundles was intertwined with the return bus to create 24 alternating dipoles and thus an $n = 24$ field error. However, at the location of the feedpoint, the dipole was not included due to space constraints which resulted in a large local $n = 1$ error field (35 G). During this past year, despite the very limited space, the feedpoint was redesigned to incorporate the “missing” dipole and the bus work to the coil was changed from a dipole to a quadrupole feed (Fig. 2).

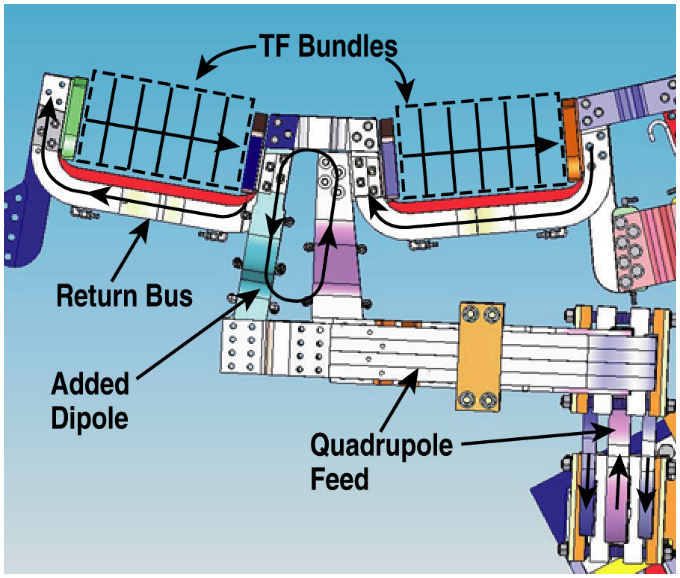

Fig. 2. Top view of the TF feedpoint. The CW arrows show the existing dipole fields that result from the return bus around the TF bundles. The CCW arrow shows the "missing" dipole field that was added in by the new bus at the feedpoint. This eliminated the large n = 1 term due to the missing dipole at this one toroidal location. The quadrupole feed can also be seen in the lower righthand corner.

The combined effect of these two changes is that two different measures of the field error were both reduced by approximately ten-fold. The local field error, i.e. that measured on the plasma boundary closest to the feed point, was reduced from 35 to 4 G. Further, the highest harmonics of the Fourier decomposition of the field averaged over a typical q = 3 surface were reduced from 1.5 G to 0.11 G. The impact on the plasma performance has been significant. On DIII–D, operation in Ohmic discharges at low density is limited by modes locking to the error field and with the new feedpoint, the lowest density achievable (without locked modes) has been reduced by 30%. In addition, recent experiments optimized the error correction algorithm using our internal coil set and have been able to further reduce our lowest density another 40% from the previous algorithm (to 0.36 x 10^{19} m^{-3} at I_p = 0.8 MA, B_T = 1 T). It is expected that this reduced error field and the reduced torque it applies will be important in the upcoming low rotation experiments.

A major element of the DIII–D program is the development of the Advanced Tokamak [7], characterized by near steady state operation at high beta and high confinement. The steady state current drive and current profile control required for an AT is provided by a combination of the self driven bootstrap current and by external current drive sources (ECCD, Fast Wave Current Drive and Neutral Beam Current Drive on DIII–D) and the beta is optimized in highly shaped, high triangularity discharges. To provide effective density control required for efficient ECCD in the highly triangular double-null divertor (DND) discharges, the lower divertor was modified. This involved the installation of a toroidally continuous, water-cooled shelf in the lower divertor region [8]. This extended the pumping aperture to an existing cryopump further inboard so that in combination with the two cryopumps located in the upper divertor region, both outer strikepoints for a highly triangular DND can be simultaneously pumped. The new structure is built from 316 SS because of its low magnetic permeability after welding and machining. The structure is designed to handle all disruption loads including a halo current up to 30% of the pre-disruption current of 3 MA with a 2:1 toroidal asymmetry. The shelf is bakeable to 400°C via a combination of inductive currents and hot air circulating through the air/water channels. The plate is protected from direct plasma impact by three rows of ATJ graphite tiles. The heat flux specification was 54 MJ to the entire plate, 27 MJ to a single row of tiles, and a triangular heat flux profile with a peak value of 9.6 MW/m^2 for 10 s with a radial width of 6.5 cm.

A major goal of the new divertor installation was to reduce carbon erosion and to improve the toroidal symmetry of the tiles and thus the carbon radiation in order to permit better comparison of diagnostic signals with modeling. To achieve this, a number of tile modifications were implemented. On the divertor shelf, through tile bolt holes were eliminated from the graphite in the high heat flux areas. Tile attachment was accomplished via bolts attached from under the shelf. On the divertor floor, new tiles were designed with a modified hold down system that removed the through tile holes from the high heat flux regions. On the centerpost, the previous tiles had flat surfaces and these tiles replaced with a new set of tiles with surfaces contoured to the radius of the inner wall. Finally, edge-to-edge alignment of all tiles was held to better than 0.1 mm with toroidal spacing between tiles decreased to less than 0.6 mm. Figure 3 shows the completed installation of the new shelf and tiles in the divertor region.

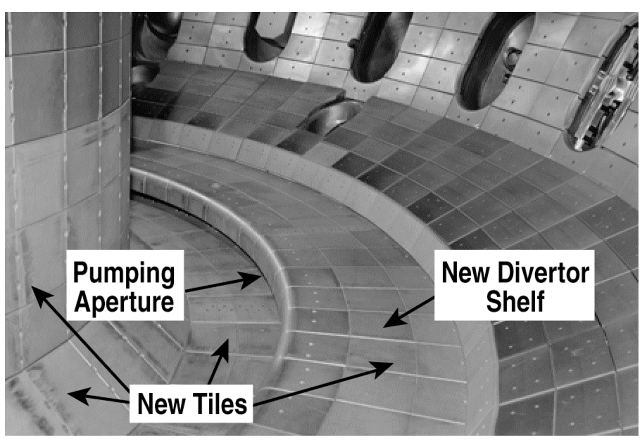

Fig. 3. New lower divertor structure showing the divertor shelf, the new floor tiles without visible bolt access holes, and the centerpost tiles. The existing cryopump is under the angled baffle plate on the outboard side.

Initial results indicate that the pump and structure are performing as expected. Vacuum tests of the lower divertor with cryopumping indicated an effective pumping speed of 18 m^3/s, consistent with design values. Effective density control of high triangularity double-null discharges was obtained using both the upper and lower cryopumps. High-power neutral beam injection with the strikepoints on both the graphite tiles on the shelf and the divertor floor have been performed and IR camera measurements of the tile surface temperatures are consistent with modeling codes used for tile design. Finally, the combined effects of eliminating exposed bolt holes and minimizing the effect of high heating at tile edges have led to a significant reduction in toroidal asymmetries. The improved toroidal symmetry can readily be seen in IR camera views of the lower divertor region [Fig. 4(a-b)].

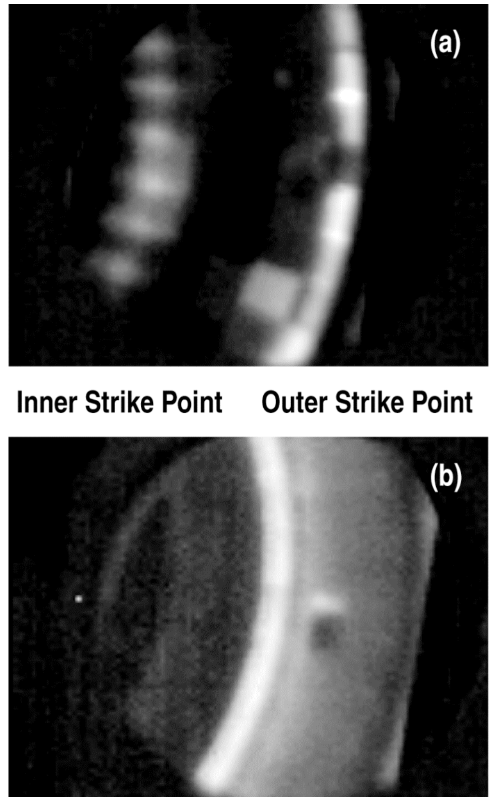

Fig. 4. IR camera view of the lower divertor region shows the significant reduction in the toroidal asymmetry in the tile heating from the (a) original divertor to the (b) new divertor with better aligned and contoured tiles.

Significant enhancements to the DIII–D PCS were completed during the LTOA period [9,10]. The PCS is a high-speed digital control system comprising 21 Intel Xeon processors with a PCI bus, running a customized Linux operating system connected by a high speed 2 GBit myrinet network. Three additional CPUs with VME access permit interaction with older components and non-PCI-based subsystems. Systems enhancements proceeding in two basic directions: higher speed and increased functionality. The higher speed was accomplished by upgrading most single Xeons to the dual CPUs, utilizing parallel processing and the use of a new series of I/O devices from D-tacq Solutions Inc. These new devices have both A/D input and D/A and digital outputs permitting a significant reduction in cycle times for feedback algorithms. In the case of RWM feedback, these new boards have reduced the algorithm cycle time from 50 to 11 μs. The enhanced functionality enabled by more CPUs and the higher processing power has been significant. The PCS now incorporates the new counter-beam CER system and computes both ion temperature and ion rotation velocity in real time (638 μs per channel), thus enabling the real-time control of plasma rotation. The new counter viewing motional Stark effect (MSE) system [11] was added with all 24 channels available for use in the real-time EFIT. Although not fully implemented, the new processors will permit the increase in the EFIT computational grid size from 33 x 33 to a 65 x 65 grid. This not only provides improved spatial resolution, but also matches the grid size used by the post-shot analysis.

Diagnostic additions and improvements were also a major focus during the LTOA. These will enhance our ability to perform in-depth AT physics, transport studies, and ITER-relevant studies. The new counter-beam MSE system will provide improved equilibrium analysis and current profile measurement [11]. The new counter-beam CER system allows more accurate measurement of low rotation velocities. The CER cross section is velocity-dependent and the ability to view the beam in both the co- and counter-direction allows an improved cross-section correction. The upgraded, high-sensitivity beam emission spectroscopy (BES) [12] system provides 30-50 times higher S/N ratio for fluctuation studies and has been expanded from 16 to 32 channels, doubling the viewing area. The relocated far-infrared scattering system [13] and mm-wave backscatter system will cover the k-spectrum range of 0-2 cm^{-1}, 7-15 cm^{-1} for the FIR and ~35-40 cm^{-1} for the backscatter and have the ability to vary the radial position of the scattered volume. Three new diagnostic systems will also provide new physics as well as address ITER-relevant issues. The new B-Stark diagnostic [14] gives an ITER-relevant alternative to determining the internal magnetic field, by measuring the Stark components from the D_α emission of the neutral beam. A dedicated fast ion profile diagnostic will provide information on the ion distribution function with a spatial resolution of ~5 cm by measuring the Doppler shift of D_α light from the charge exchange light from fast neutrals. Finally, two quartz microbalance diagnostic systems [15] in the lower divertor will help diagnose carbon migration.

One of the major limitations to long-pulse operation of DIII–D has been the poorly cooled interconnecting and return bus of the toroidal field coil. The installation of a cooling plate and reconfiguration of the cooling water flow paths should double the pulse length at full field to ~10 s. Figure 5 shows the improved temperature performance of this component after the upgrade. More than half of 48 bus sections have been upgraded with these new plates and work will continue throughout the year until completion.

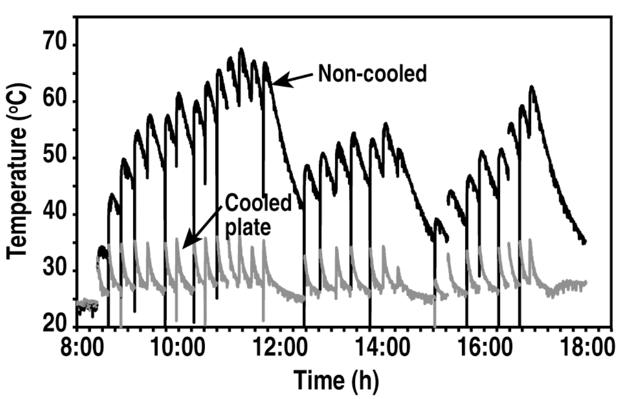

Fig. 5. The use of a cooled plate on the interconnecting buswork for the TF coil has significantly reduced the peak temperature for this assembly and will permit more than a doubling of the pulse length capability for the toroidal field. The cooling plate eliminates the ratcheting effect seen in the our typical 12-15 minute cycle time.

3. SUMMARY

A number of significant enhancements to the DIII–D device and facility were completed during the one year shutdown following April 2005. The major upgrades including the new counter beam capability and lower divertor structure, coupled with the upgraded PCS, new diagnostic capability, and other system enhancements have opened up new research regimes to pursue AT studies, basic transport physics, and ITER-relevant issues. Completion of further upgrades to the EC system and TF coil cooling should further enhance DIII–D capability to address steady state/long pulse issues relevant to ITER and Advanced Tokamak operation.

REFERENCES

[1] J.T. Scoville et al., Simultaneous feedback control of plasma rotation and stored energy on the DIII–D tokamak, this conference.

[2] K.H. Burrell, D.H. Kaplan, P. Gohil, et. al., Rev. Sci. Instrum. 72 (2001) 1028; K.H. Burrell, P. Gohil, R.J. Groebner, et. al., Rev. Sci. Instrum. 75 (2004) 3455.

[3] A.M. Garofalo, T.H. Jensen, L.C. Johnson, et al., Sustained rotational stabilization of DIII–D plasmas above the no-wall beta limit, Phys. Plasma 9 (2002) 1997.

[4] D.A. Humphreys, J.R. Ferron, R.J. La Haye, T.C. Luce, C.C. Petty, R. Prater, A.S. Welander, Active control for stabilization of neoclassical tearing modes, Phys. Plasmas 13 (2006) 56113

[5] R.J. La Haye, R. Prater, R.J. Buttery, N. Hayashi, A. Isayama, M.E. Maraschek, L. Urso, H. Zohm, Cross-machine benchmarking for ITER of neoclassical tearing mode stabilization by electron cyclotron current drive, Nucl. Fusion 46 (2006) 45.

[6] K.H. Burrell, Quiescent double barrier mode in the DIII–D tokamak, Phys. Plasmas 8 (2001) 2153; K.H. Burrell, W.P. West, E.J. Doyle, et al., Edge radial electric field structure in quiescent H-mode plasma in the DIII–D tokamak, Plasma Physics Contr. Fusion 46 (2004) A165.

[7] C.M. Greenfield et al., Advanced tokamak research in DIII-D, Plasma Phys. Control. Fusion 46 (2004) B213.

[8] P.M. Anderson et al., Design, fabrication, and installation of the lower divertor for DIII–D, this conference.

[9] D.A. Piglowski, et al., Enhancements in the second generation DIII–D digital plasma control system, this conference.

[10] B.G. Penaflor, et al., Special Issue, Fusion Engin. Design. 71 (2004) 47.

[11] C.T. Holcomb et al., Motional Stark effect diagnostic expansion on DIII–D for enhanced current and Er profile measurements, 16th Conf. on High-Temperature Plasma Diagnostics (HTPD) 2006 to be published in Rev. Sci. Instrum.

[12] G.R. McKee, R.J. Fonck, D.K. Gupta, D.J. Schlossberg, M.W. Shafer, accepted for publication in Rev. Sci. Instrum. (2006).

[13] T.L. Rhodes, et al., Rev. Sci. Instrum., accepted for publication, 2006.

[14] W. Mandl et al., Plasma Phys. Contr. Fusion 35 (1993) 1373.

[15] H.G. Esser et al. Fusion Engin. Design 66-68 (2003) 855-860; H.G. Esser et al. Physica Scripta T111 (2004) 129-132.

ACKNOWLEDGMENT

This is a report of work supported by the U.S. Department of Energy under Cooperative Agreement DE-FC02-04ER54698.